

CIECAM16-based Tone Mapping of High Dynamic Range Images

Imran Mehmood, Miaosen Zhou, Muhammad Usman Khan and Ming Ronnier Luo; State Key Laboratory of Extreme Photonics and Instrumentation, Zhejiang University, Hangzhou, China.

Abstract

A significant challenge in tone mapping is to preserve the perceptual quality of high dynamic range (HDR) images when mapping them to standard dynamic range (SDR) displays. Most of the tone mapping operators (TMOs) compress the dynamic range without considering the surround viewing conditions such as average, dim and dark, leading to the unsatisfactory perceptual quality of the tone mapped images. To address this issue, this work focuses on utilizing CIECAM16 brightness, colorfulness, and hue perceptual correlates. The proposed model compresses the perceptual brightness and transforms the colors from HDR images using CIECAM16 color adaptations under display conditions. The brightness compression parameter was modeled via a psychophysical experiment. The proposed model was evaluated using two psychophysical experimental datasets (Rochester Institute of Technology (RIT) and Zhejiang University (ZJU) datasets).

Introduction

High dynamic range (HDR) imaging offers an extensive tonal range and prioritizes the preservation of intricate details, providing a high level of visual engagement in data visualization. However, the mainstream consumer capturing and display devices lack the requisite capabilities to handle such visually complex content. A TMO adjusts the tonal range of HDR data to match the capabilities of the device before displaying. While this reduction in the tonal range can lead to low perceptual quality of tone mapped images [1].

Over the years, several TMOs have been proposed in the literature [2-5]. Previous TMOs typically focused on compressing either the luminance channel of HDR images such as Drago [6] and Khan [5] TMOs; individual R, G, B channel compression such as Reinhard's TMO [7]; or individual X, Y, and Z coordinates such as iCAM06 [8]. The luminance compression by preserving chromaticity coordinates introduces smaller hue shifts with over-saturated pixels. The separate processing of the three-color channels can lead to high quantification due to color balance issues.

The HVS is significantly influenced by the viewing conditions, such as luminance and colorimetry characteristics of the light source. Color appearance models (CAMs), such as CIECAM02 [9], CIECAM16 [10] and ZCAM [11], integrate the cone and rod responses in a series of computational procedures that incorporate chromatic adaptation and tone compression. Chromatic adaptation facilitates the transformation of the colors in an input image to align with those perceived under a specific viewing condition.

The recently standardized CIECAM16 integrates HVS phenomena to more accurately predict color appearance, encompassing chromatic adaptation, nonlinear response, and opponent color theory. It is known that when luminance is compressed for tone mapping the saturation of the output images is increased. However, when the brightness in CIECAM16 is compressed; yet preserving colorfulness and hue, the colors shift out-of-gamut due to crosstalk between brightness and chroma



Figure 1. The brightness compressed HDR images from (a) least compressed to (d) most compressed.

(or colorfulness). Figure 1 shows the color distortions that occurred during brightness compression in CIECAM16.

In this paper, a tone mapping model (TMO_z) is proposed that utilizes perceptual correlates of CIECAM16 to compress the perceptual brightness and perform image appearance mapping based on colorfulness and hue. It involves compression of brightness after separating it into base and detail layers. Subsequently, the local contrast is enhanced and new colorfulness and hue are derived using CIECAM16 color adaptation equations. The brightness compression parameter is automated through a psychophysical experiment. The visual results along with performance comparison using psychophysical experiments are presented.

Tone Mapping Model

The flowchart of the TMO_z is depicted in Figure 2. The input to the TMO_z is XYZ HDR (X_H, Y_H, Z_H) data. The RGB to XYZ transformation can be achieved by employing a camera characterization model or color space conversion matrix without non-linearizing the gamma mapping.

The determination of perceptual correlates in CIECAM16 requires surround conditions to accurately determine the perceptual attributes. There are two types of surround conditions to be used in the TMO_z i.e., one for computing the brightness of the HDR image using the adaptation luminance (L_{aH}), background luminance (Y_{bH}), and white point (X_{wH}, Y_{wH}, Z_{wH}), the other for computing the hue and colorfulness from the HDR image under display conditions using adaptation luminance (L_{ad}), background luminance (Y_{bd}), and white point (X_{wd}, Y_{wd}, Z_{wd}).

CIECAM16 BRIGHTNESS CALCULATION

The algorithm starts with calculations of standard CIECAM16 parameters. Firstly, calculate the input parameters using HDR white point (X_{wH}, Y_{wH}, Z_{wH}) as follows.

$$\begin{pmatrix} R_{wH} \\ G_{wH} \\ B_{wH} \end{pmatrix} = M_{CAT16} \begin{pmatrix} X_{wH} \\ Y_{wH} \\ Z_{wH} \end{pmatrix} \quad (1)$$

where M_{CAT16} is the CAT16 chromatic adaption matrix. Now, calculate the degree of adaptation, D_H .

$$D_H = F \left[1 - \left(\frac{1}{3.6} \right) \right] \exp \left(\frac{-L_{aH} - 42}{92} \right) \quad (2)$$

$$D_H = F \left[1 - \left(\frac{1}{3.6} \right) \right] \exp \left(\frac{-L_{aH} - 42}{92} \right) \quad (3)$$

Calculate other parameters as follows

$$D_{RH} = D_H \frac{Y_{wH}}{R_{wH}} + 1 - D_H \quad (4)$$

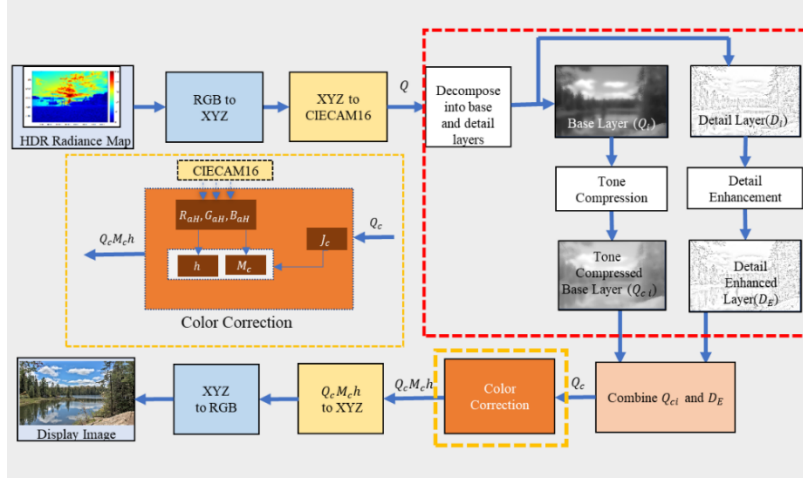


Figure 2. The workflow of the present proposed TMO.

Similarly, calculate D_{BH} and D_{GH} by replacing R_{wH} by B_{wH} and G_{wH} , respectively. Calculate,

$$\begin{pmatrix} R_{wCH} \\ G_{wCH} \\ B_{wCH} \end{pmatrix} = \begin{pmatrix} D_R R_{wH} \\ D_G G_{wH} \\ D_B B_{wH} \end{pmatrix} \quad (5)$$

$$R_{awH} = 400 \left(\frac{\left(\frac{F_{LH} R_{wCH}}{100} \right)^{0.42}}{\left(\frac{F_{LH} R_{wCH}}{100} \right)^{0.42} + 27.13} \right) + 0.1 \quad (6)$$

Calculate the achromatic response for the white point.

$$A_{wH} = [2R_{awH} + G_{awH} + 0.05B_{awH} - 0.305]N_{bb} \quad (7)$$

Now apply the formulation on HDR image XYZ (X_H, Y_H, Z_H) as follows.

$$\begin{pmatrix} R_H \\ G_H \\ B_H \end{pmatrix} = M_{CAT16} \begin{pmatrix} X_H \\ Y_H \\ Z_H \end{pmatrix} \quad (8)$$

Calculate the color adaptation for the HDR image.

$$\begin{pmatrix} R_{CH} \\ G_{CH} \\ B_{CH} \end{pmatrix} = \begin{pmatrix} D_{RH} R_H \\ D_{GH} G_H \\ D_{BH} B_H \end{pmatrix} \quad (9)$$

Calculate the post-adaptation cone responses for the HDR image.

$$R_{aH} = \begin{cases} -400 \left(\frac{(-F_{LH} R_{CH}/100)^{0.42}}{(-F_{LH} R_{CH}/100)^{0.42} + 27.13} \right) + 0.1, & R_{CH} < 0 \\ 400 \left(\frac{(F_{LH} R_{CH}/100)^{0.42}}{(F_{LH} R_{CH}/100)^{0.42} + 27.13} \right) + 0.1, & R_{CH} \geq 0 \end{cases} \quad (10)$$

Similarly, B_{aH} and G_{aH} can be computed by replacing R_{CH} with B_{CH} and G_{CH} , respectively. The chromatic response is computed as follows.

$$A_H = [2R_{aH} + G_{aH} + 0.05B_{aH} - 0.305]N_{bb} \quad (11)$$

and the lightness is given by (12).

$$J_H = 100 \left(\frac{A_H}{A_{wH}} \right)^{c.z} \quad (12)$$

The absolute predictor of the brightness of the HDR image is computed as

$$Q = (4/c) \sqrt{J_H/100} \times (A_{wH} + 4) F_{LH}^{0.25} \quad (13)$$

The brightness Q is further normalized with the maximum brightness of the image (Q_{max}) and decomposed into the base (Q_i) and detail (D_i) layers to preserve and enhance the local contrast. Separating the brightness into two layers also diminishes the halo artifacts arising due to spatial tone mapping. The tone compression is applied on the base layer while the detail layer is

further enhanced to increase the local contrast of the resultant image. The images can be decomposed into detail and base layers by subtracting a filtered image from the original image. The edge-preserving nonlinear Bilateral filter is used to filter the Q with the default parameters [12].

Brightness Compression

In traditional TMOs, the luminance channel is often compressed while the chromatic coordinates are preserved, which can lead to hue shifts and over-saturation of the tone-mapped image. In TMO_z, the base layer of the brightness image is utilized for compression. Since, the conversions involved in CIECAM16 can be computationally expensive, therefore, to manage the processing time effectively, a simplified power function is used to compress brightness as follows.

$$Q_{ci} = A (Q_i)^\gamma \quad (14)$$

The scaling factor A is set to 1. The parameter γ represents the curve-shaping parameter that controls the degree of brightness compression. By adjusting the value of γ , the compression of brightness can be increased or decreased, impacting the overall tone mapping effect. The γ is predicted automatically based on the HDR image characteristics. The modeling of γ prediction is discussed in subsequent sections.

Local Contrast Enhancement

The preservation of high-frequency information in the HDR image is achieved through the separation of the base and detail layers. This process ensures that fine details are retained. As the base layer undergoes compression, the information contained in its low-frequency components is suppressed. To address this issue, the tone mapped base layer and the preserved detail layer are transformed back. However, this transformation alone does not provide sufficient local contrast in the image. To enhance the local contrast, the following equation is employed.

$$D_E = D_{i,max} \left(\frac{|D_i|}{D_{i,max}} \right)^\beta \times \text{sign}(D_i) \quad (15)$$

Where $D_{i,max}$ is the maximum value of $|D_i|$. The user parameter β controls the local contrast by either stretching or reducing the high-frequency content. Authors note the best local contrast when β ranges 1.1 to 1.3. In this study, $\beta = 1.1$ was used.

The final tone compressed brightness is computed by combining the tone-compressed brightness base layer Q_{ci} and the enhanced detail layer D_E i.e., $Q_c = Q_{max} (Q_{ci} \cdot D_E)$.

COLORFULNESS AND HUE CALCULATION

The hue of the tone-mapped image can directly be computed from the HDR image, utilizing the same HDR surround conditions. As mentioned earlier, human vision is influenced by viewing conditions, with the colorimetric information of the surroundings significantly affecting the visual adaptation mechanism. Therefore, the colorfulness of an object is dependent on factors such as illumination, background luminance, adaptation luminance, and other variables. In the CIECAM16 color model, there exists a relationship between colorfulness and brightness, leading to colorfulness distortions when compressing the brightness of the HDR image.

Additionally, the brightness of the HDR image was normalized before separating it into the base and detail layers. This normalization process alone preserves the colorfulness of the HDR image for the tone-compressed brightness, resulting in an image with reduced colorfulness (in contrast to typical tone mapping operators where saturation increases when luminance is compressed), as shown in Figure 4 (a). Consequently, a new method for determining colorfulness is required for compressed brightness.

The new colorfulness is obtained by applying human visual system (HVS) chromatic adaptation using the CIECAM16 specified. The hue angle can then be calculated using the following formula.

$$a_H = R_{aH} - \frac{12 \cdot G_{aH}}{11} + \frac{B_{aH}}{11}$$

$$b_H = \frac{R_{aH} + G_{aH} - 2B_{aH}}{9} \quad (16)$$

$$h_H = \tan^{-1}(b_H/a_H) \quad (17)$$



Figure 4: (a) The tone mapped image using the colorfulness of the original HDR image. (b) The image with the new colorfulness estimation.

Compute the Colorfulness

To calculate the colorfulness, first calculate the achromatic response A_{wd} and F_{Ld} corresponding to the display white point (X_{wd}, Y_{wd}, Z_{wd}) using display surround conditions, including the adaptation luminance L_{Ad} and background luminance Y_{bd} , following equations (1) to (7).

Next, determine the lightness and colorfulness of the tone-mapped image by using the tone-compressed brightness Q_c and A_{wd} with the following formulae.

$$J_c = 6.25 \cdot \left[c \cdot \frac{Q_c}{[A_{wd} + 4] F_{Ld}^{0.25}} \right]^2 \quad (18)$$

$$e_t = \frac{1}{4} \cdot \left[\cos\left(\frac{h_H \pi}{180} + 2\right) + 3.8 \right] \quad (19)$$

$$t = \frac{\left(\frac{50000}{13} \cdot N_c \cdot N_{cb}\right) \cdot e_t \cdot (a_H^2 + b_H^2)^{1/2}}{R_{aH} + G_{aH} + \left(\frac{23}{20}\right) \cdot B_{aH}} \quad (20)$$

$$C_c = t^{0.9} \left(\frac{J_c}{100}\right)^{0.5} (1.64 - 0.29^n)^{0.73} \quad (21)$$

$$M_c = C_c F_{Ld} \quad (22)$$

where the value of c, N_c, N_{cb} are the same as in standard CIECAM16. The image with the new color estimation is depicted in Figure 4 (b). It can be seen that when the hue and colorfulness are calculated by employing the proposed method, the colors are restored in the tone mapped image.

Display Image Transformation

Finally, the brightness, colorfulness, and hue (Q_c, M_c, h_H) are transformed into XYZ coordinates using the inverse CIECAM16 model [10]. The inverse transformation considers the display surround conditions. To simulate incomplete light adaptation and the glare in visual system, 1% of the pixels are clipped. The resulting XYZ image is then transformed into RGB images using the XYZ to sRGB transformation or a particular display characterization model, such as the GOG model. In this paper, the images are presented in the sRGB color space.

Brightness Compression Parameter Modeling

The brightness Q of the HDR image was compressed using (14) with a control parameter γ . This parameter was modeled in a psychophysical experiment to automate the process of tone mapping. The key of an image (k), is a statistical parameter that quantifies the overall brightness of the image [3]. A bright image will have a relatively higher key compared to a darker image. The control parameter γ can be expressed as follows.

$$\gamma = f(k) \quad (23)$$

where $f(\cdot)$ is some function to be modeled psychophysically such that the γ is calculated automatically using the k .

Over 300 HDR images were assessed from various datasets, including RIT, Stanford, Funt, and ZJU. To ensure diversity, 30 images with the lowest and highest key values from the RIT dataset were selected. These images covered a range of scenes, buildings, color charts, and objects captured at different times. γ values for each HDR image were optimized for the best tone-mapped results. Each image was rendered with five γ levels (± 0.1 and ± 0.2), resulting in a total of 150 images. To assess variance, 30% of the images were repeated, totaling 225 images for the experiment.

The experiment was conducted in a dark room following the ITU recommendations [13]. Ten observers participated in the experiment from various disciplines with mean age 26 and standard deviation (SD) of 2.4. The mean and SD of inter-observer variance were 21 and .85 whereas the intra-observer values were 18 and 1.65, respectively.

The data from the experiment was analyzed to model the curve shaping parameter γ . The percentage of preferred images was calculated and γ values at 50% were selected for modeling. In a pair of two images displayed to the subject, the selected image was considered the preferred image over the other image in that pair. Linear regression was applied to the following model.

$$\gamma = ak + b \quad (24)$$

where the constants a and b optimized using regression are 0.6781 and 0.3128, respectively. Figure 5 shows the correlation between experimental values and model values. The R^2 was 0.82, which implied that the model performance agreed well with the psychophysical data. Hence, the tone compression of brightness was made adaptive using this model.

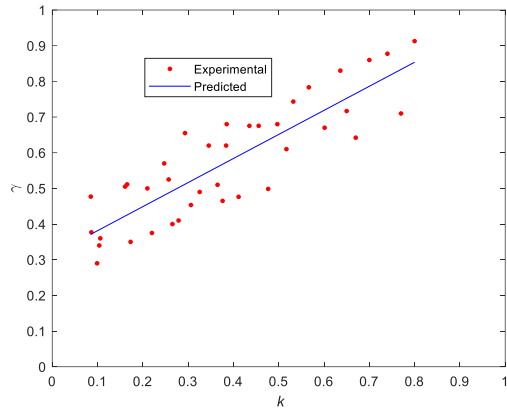


Figure 5: The correlation between experimental and prediction values.

Results

VISUAL COMPARISON

Following the recommendations of Fairchild [14] and Luo [15], the images were processed with L_{AH} set to 20% of the maximum luminance in the HDR image multiplied by 10,000, $L_{AD} = 100$, $Y_b=20$, and D65 white point with average surround, for both HDR and tone-mapped images.

The performance of the TMO_z was compared with state-of-the-art TMOs. The TMOs include three recent TMOs named Hui

[16], Liang [4] and Khan [5]; four widespread TMOs [17], iCAM06 [8], Schlick [2] and Reinhard [3] and one TMO from 2006 named Meylan TMO [18]. Since the TMO_z was fully adaptive, the default parameters (as suggested in the original papers) were used for other TMOs. Figures 6 and 7 visually compare the TMOs, including TMO_z . Each figure contains a linearly scaled HDR image to visualize the dynamic range of the HDR image. In Figure 6, images contain two Macbeth ColorChecker charts and a bull placed in highlights and shadow areas, respectively. It is clear from Figure 6 that other TMOs could not produce desired colors. Moreover, the ColorChecker in the highlight region is not properly exposed. TMO_z produced well details and color in shadows as well as highlight regions. It is noted that human vision experiences low colorfulness or chroma in dark or dim lighting conditions. This effect is visible in the dark regions, especially in the colors of the ColorChecker chart placed in the shadows can be noticed revealing the HVS phenomenon. Hui produced relatively more colorfulness in color checker chart. The images tone mapped using Hui's and Liang's TMO suffer from colorfulness distortions and hue shifts that can be noticed in the ColorChecker chart. Meylan produces images with very low colorfulness.

Similarly, Figure 7 shows that the TMO_z accomplishes significant balance among details, contrast, and colorfulness. The hue and colorfulness distortions are apparent in iCAM06. The other TMOs also have either hue, colorfulness or contrast distortions.

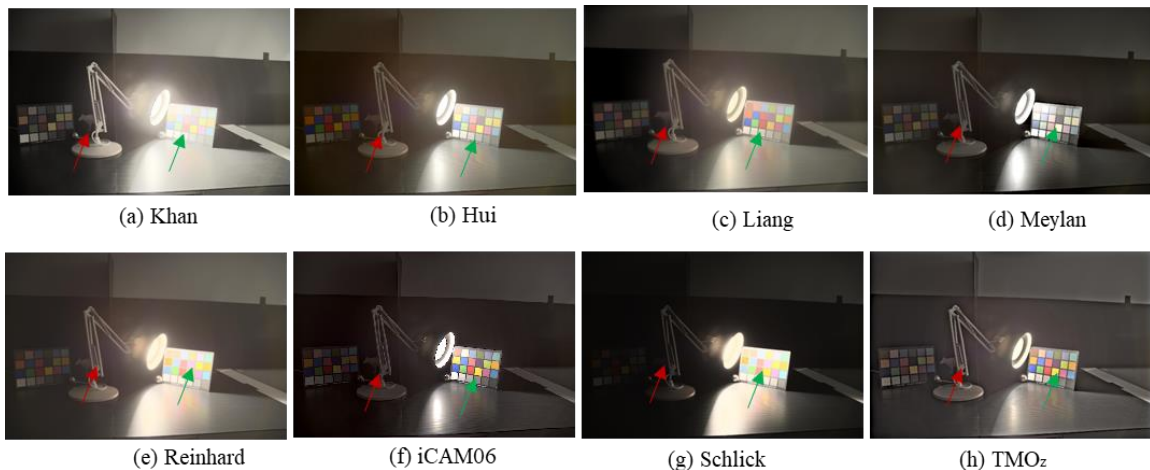


Figure 6. TMO_z compared with the various TMOs. The ColorChecker chart reveals that TMO_z produces better color reproduction.

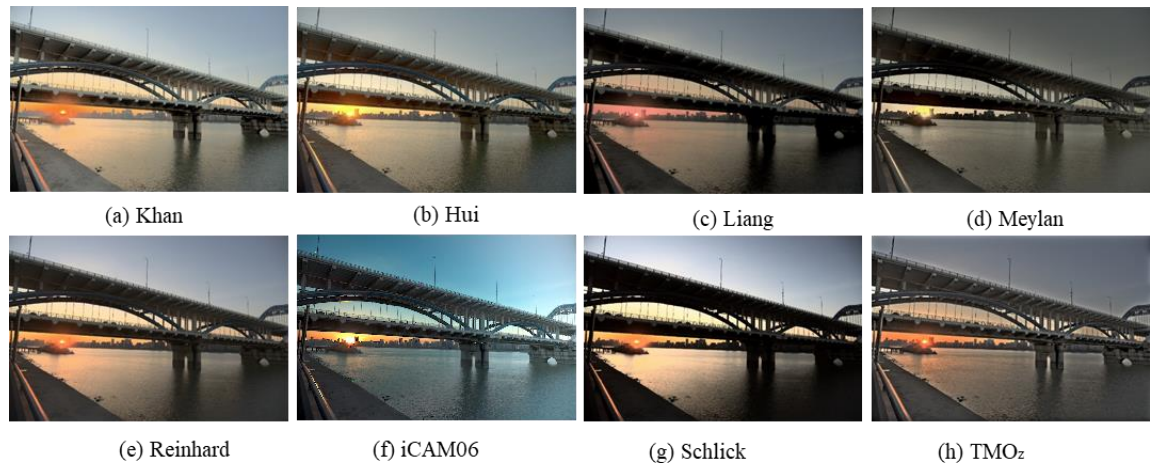


Figure 7. TMO_z compared with the various TMOs. TMO_z reproduces details in shadows and highlights better than other TMOs.

Performance Comparison Using Psychophysical Experiments

To test the performance of the TMOz two psychophysical experiments were conducted. In the first experiment, TMOz was compared with state-of-the-art TMOs. Ten HDR images from the RIT database were used in a pair comparison experiment. These images were entirely different from the images used in γ modelling experiment. Images were assessed using three scales: contrast, colorfulness, and overall preference. Most TMOs do not consider display dynamic range and other factors, images were not assessed in overall preference for contrast and colorfulness. Rather the images were assessed in the following way.

1. Which image has more contrast?
2. Which image has more colorfulness?
3. Which image do you prefer based on overall preference?

Ten images as depicted in Figure 9, were tone mapped with the seven TMOs and transformed using the Apple Pro XDR display characteristics model. The total number of tone mapped images was 70. Since the same display was used in the current experiment which was used previously, similar experimental conditions were applied. The total number of pairs for comparison was 10 (images) $7 \times (\text{TMOs}) \times (6)/2 + 30\%$ repetitions = 273.

Ten subjects performed the experiment in three sessions to assess the image quality in terms of three scales. All the subjects were students of the university working in optical science. Specifically, four females and six males performed the experiment with a mean age of 25 and an SD of 2.5. The average time taken by a subject to perform the entire experiment was approximately 50 minutes. The average inter- and inter-observer variability were 28.73 and 20.56 with SD values of 3.29 and 7.36, respectively.

The raw data from the experiment was converted into standardized Z-scores. Figures 10-12 represent the comparisons of various TMOs for contrast, colorfulness, and overall preference scales, respectively. The error bars represent 95% confidence interval. Figure 10 showed that Schlick's and Liang's TMOs had the highest contrast scores for each tone mapped image. Meylan's TMO had the lowest contrast values for all of the images. Few images tone mapped using Reinhard TMO had higher scores than the mean value while other images had lower scores. The TMOz achieved moderate contrast for most images and ranked in the middle of these TMOs. Most images of TMOz had higher contrast than Khan's, Hui's and Meylan's TMOs, while it was lower than Reinhard's, Liang's and Schlick's images.

Figure 11 shows the standardized subjective scores of the colorfulness scales for various TMOs. Again, the scores of TMOz for all images ranked in the middle. The Hui's TMO produced the highest colorfulness images. Nine images out of ten were ranked with the highest colorfulness. Khan's TMO had similar behavior and all the images had higher colorfulness when compared to the other tone mapped images.

It can be seen from Figures 10 and 11 that Schlick's and Liang's TMOs had the highest contrast, respectively, but had the lowest colorfulness. Hui's and Khan's TMOs had similar behavior; these TMOs attained lower contrast scores while having the highest colorfulness scores. Meylan's TMO manages the saturation in its algorithm but overly reduces the colorfulness. Reinhard's TMO produces slightly higher saturated colors as discussed in [1]. The TMOz achieved the ranking in the middle. The images produced by TMOz had colorfulness slightly lower than Reinhard's TMO but higher than Schlick's, Liang's and



Figure 9. Images used for the first psychophysical experiment, to compare TMOz with other TMOs.

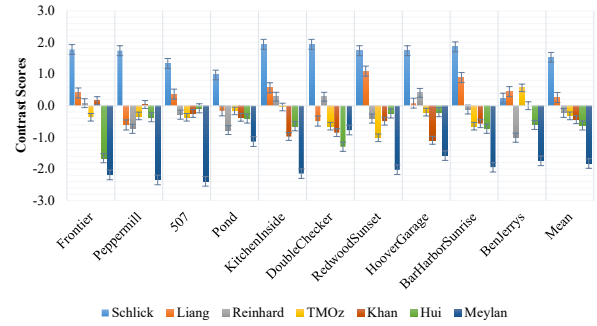


Figure 10. The performance of TMOs in terms of contrast scale using the first psychophysical experiment.

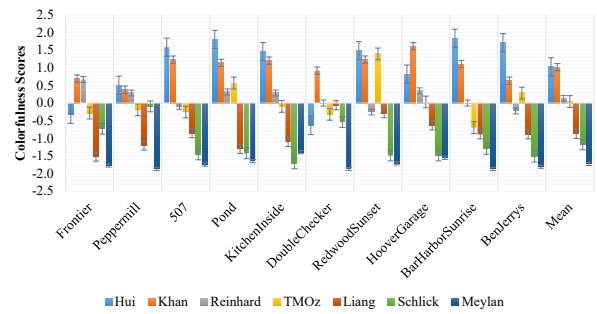


Figure 11. The performance of TMOs in terms of colorfulness scale using the first psychophysical experiment.

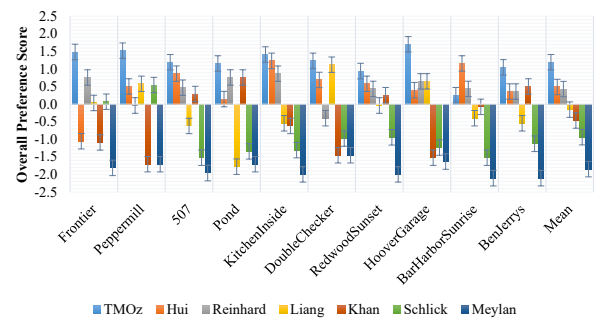


Figure 12. The performance of TMOs in terms of overall preference scale using the first psychophysical experiment.

Meylan's TMOs. It conveyed that the images tone mapped using TMOz had moderate colorfulness. The colorfulness for the TMOz was adapted from the HDR image using CIECAM16 color adaption equations and display surround conditions. Hence, it can be stated that the images reproduced using TMOz have more optimal colorfulness for HDR and tone mapping applications.

Finally, the standardized subjective scores overall preference are reported in Figure 12. The TMOz outperformed all of the TMOs in comparison. The colorfulness and contrast of the TMOz images were moderate; hence it is assertive that the subjects preferred TMOz while comparing the other image in the pair.

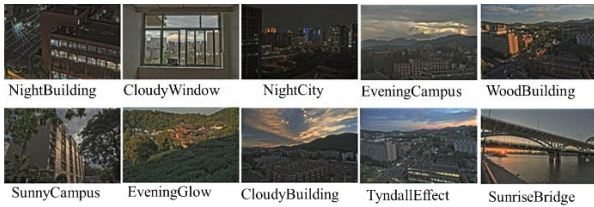


Figure 13. Images used for the second psychophysical experiment, to compare TMO_z with other $TMOs$.

In the second performance comparison psychophysical experiment, TMO_z was compared with the same $TMOs$ in terms of overall preference using ZJU HDR dataset. The ZJU HDR dataset includes 50 outdoor and indoor HDR images. A full-frame SONY ILCE-7RM3 camera was used to capture nine multiple exposures for each HDR scene by bracketing. The raw image files were then processed to create the HDR images using the "Merge to HDR Pro" function in Adobe Photoshop 2023. Ten HDR images included for the rendering purpose are depicted in Figure 13. The images were tone mapped with the seven $TMOs$ and transformed using the Apple Pro XDR display characteristics model. The total number of tone mapped images was 70. The total number of pairs for comparison was $10 \text{ (images)} \times 7 \text{ (TMOs)} \times (6)/2 + 20\% \text{ repetitions} = 253$. Ten subjects participated in the experiment with a mean age of 24 and SD 1.2. The intra- and inter-observer variability were 17.75 and 15.89 with SD of 5.18 and 5.86, respectively.

The standardized subjective scores for overall preference showed that TMO_z gave the best overall ranking which agreed with the first performance comparison experiment. The consistency was determined using the SD values of each TMO . The TMO_z also achieved the highest consistency with SD equal to 0.216, Schlick's TMO had the lowest consistency with 0.84. Hui, Reinhard, Liang, Khan and Meylan had 0.47, 0.37, 0.65, 0.40 and 0.65, respectively.

Conclusions

A CIECAM16-based tone mapping model for HDR imaging was developed. The model tone maps the low-frequency components of the perceptual brightness while enhancing the high-frequency components using base and details layers of the brightness. The model adapts the colorfulness and hue from the HDR image using CIECAM16 color adaptation equations, ensuring more precise colors in the tone mapped image. One psychophysical experiment was conducted to model the brightness compression parameter and two psychophysical experiments were conducted to test the performance of the TMO_z with other state-of-the-art $TMOs$ such as Hui, Liang, Reinhard, Khan, Schlick and Meylan.

The performance of TMO_z was assessed using three scales, i.e., contrast, colorfulness and overall preference. The TMO_z ranked in the middle for contrast and colorfulness scales, asserting that the TMO_z had moderate contrast and more precise colorfulness. The TMO_z outperformed the other $TMOs$ in the study in the overall preference scale.

References

[1] A. Artusi, T. Pouli, F. Banterle, and A. O. Akyüz, "Automatic saturation correction for dynamic range management algorithms," *Signal Processing: Image Communication*, vol. 63, pp. 100-112, 2018.

[2] C. Schlick, "Quantization techniques for visualization of high dynamic range pictures," in *Photorealistic rendering techniques*: Springer, 1995, pp. 7-20.

[3] E. Reinhard, M. Stark, P. Shirley, and J. Ferwerda, "Photographic tone reproduction for digital images," in *Proceedings of the 29th annual conference on Computer graphics and interactive techniques*, pp. 267-276, 2002.

[4] Z. Liang, J. Xu, D. Zhang, Z. Cao, and L. Zhang, "A hybrid 11-10 layer decomposition model for tone mapping," in *Proceedings of the IEEE conference on computer vision and pattern recognition*, pp. 4758-4766, 2018.

[5] I. R. Khan, W. Aziz, and S.-O. Shim, "Tone-mapping using perceptual-quantizer and image histogram," *IEEE Access*, vol. 8, pp. 31350-31358, 2020.

[6] F. Drago, K. Myszkowski, T. Annen, and N. Chiba, "Adaptive logarithmic mapping for displaying high contrast scenes," in *Computer graphics forum*, pp. 419-426, 2003.

[7] E. Reinhard and K. Devlin, "Dynamic range reduction inspired by photoreceptor physiology," *IEEE transactions on visualization and computer graphics*, vol. 11, no. 1, pp. 13-24, 2005.

[8] J. Kuang, G. M. Johnson, and M. D. Fairchild, "iCAM06: A refined image appearance model for HDR image rendering," *Journal of Visual Communication and Image Representation*, vol. 18, no. 5, pp. 406-414, 2007.

[9] N. Moroney, M. D. Fairchild, R. W. Hunt, C. Li, M. R. Luo, and T. Newman, "The CIECAM02 color appearance model," in *Color and Imaging Conference*, pp. 23-27, 2002.

[10] C. Li *et al.*, "Comprehensive color solutions: CAM16, CAT16, and CAM16-UCS," *Color Research & Application*, vol. 42, no. 6, pp. 703-718, 2017.

[11] M. Safdar, J. Y. Hardeberg, and M. Ronnier Luo, "ZCAM, a colour appearance model based on a high dynamic range uniform colour space," *Optics Express*, vol. 29, no. 4, pp. 6036-6052, 2021/02/15 2021.

[12] F. Durand and J. Dorsey, "Fast bilateral filtering for the display of high-dynamic-range images," in *Proceedings of the 29th annual conference on Computer graphics and interactive techniques*, pp. 257-266, 2002.

[13] I. Recommendation, "Methodologies for the subjective assessment of the quality of television images," *International Telecommunication Union*, pp. 500-14, 2020.

[14] M. D. Fairchild, "A revision of CIECAM97s for practical applications," *Color Research & Application: Endorsed by Inter-Society Color Council, The Colour Group (Great Britain), Canadian Society for Color, Color Science Association of Japan, Dutch Society for the Study of Color, The Swedish Colour Centre Foundation, Colour Society of Australia, Centre Français de la Couleur*, vol. 26, no. 6, pp. 418-427, 2001.

[15] M. R. Luo and C. Li, "CIECAM02 and its recent developments," *Advanced color image processing and analysis*, pp. 19-58, 2013.

[16] H. Li, X. Jia, and L. Zhang, "Clustering based content and color adaptive tone mapping," *Computer Vision and Image Understanding*, vol. 168, pp. 37-49, 2018.

[17] I. Mehmood, X. Liu, M. U. Khan, and M. R. Luo, "Method for developing and using high quality reference images to evaluate tone mapping operators," *JOSA A*, vol. 39, no. 6, pp. B11-B20, 2022.

[18] L. Meylan and S. Susstrunk, "High dynamic range image rendering with a retinex-based adaptive filter," *IEEE Transactions on image processing*, vol. 15, no. 9, pp. 2820-2830, 2006.